Preliminary Results Combining Ground-based RAMAN Lidar and NAST-I Airborne Spectrometer to Describe the Evolution of a Cirrus Cloud – EAQUATE, ITALY 2004

Maestri Tiziano[1], Rizzi Rolando[1]
Di Girolamo Paolo[2], Summa Donato[2]
Romano Filomena[3]

[1]ADGB- Physics Department – Alma Mater Studiorum, University of Bologna , Bologna (Italy)
[2]DIFA - Dip. di Ingegneria e Fisica dell'Ambiente – University of Basilicata, Potenza (Italy)
[3]IMAA - Istituto di Metodologie per l'Analisi Ambientale - CNR , Potenza (Italy)

Abstract

In the evening of Sept. 6, 2004, as part of the Southern Italy Eaquate campaign, the Proteus aircraft flew four times over a moderately thick high cirrus cloud in the Potenza region, southern Italy. The evolution of the cloud was monitored by the DIFA Raman lidar ground station in Potenza and four radiosondes were released from the IMAA ground station (8 km far from the DIFA location), both providing potentially an excellent description of the atmospheric gaseous and particulate state. The general evolution of the cloud field was monitored using MSG infrared images, available every 15 minutes.

Among the instrument flying on Proteus, the sensor NAST-I is used to compare with accurate radiance simulations based on the description provided by the ground based instrumentation and radiosondes. Considered the quality of the comparison among simulated and measured radiances, the vertical structure of fluxes and cooling/heating rates is computed thus providing a link between the measured state and the time evolution of the cirrus cloud.

Introduction

Data analyzed in this work were collected during the Italian phase (first phase from 5th - 10th September 2004) of the international field experiment campaign called Eaquate. A second phase of the experiment took place in the UK (13th - 22nd September 2004). The Eaquate campaign was designed to study the atmosphere using aircraft and ground based instruments, demonstrating the benefit of these measurements in validating hyperspectral satellite sounding observations. The Proteus high altitude aircraft participated in both campaigns, providing measurements from the NAST thermal infrared interferometer and microwave radiometer, the Scanning HIS infrared interferometer, the FIRSC far-IR interferometer, and the micro-MAPS CO sensor. The Italian phase, funded by the Integrated Program Office and by the Province of Benevento, was carried out within an international collaboration between NASA Langley Research Center, University of Wisconsin, the Istituto di Metodologie per l'Analisi Ambientale (IMAA-CNR), the Mediterranean Agency for Remote Sensing (MARS) and the Universities of Basilicata and Napoli. The experiment involved a range of ground based remote sensing instruments (lidars, microwave radiometer, infrared interferometer, ceilometer) as well as an Earth Observing System-Direct Readout Station. [http: //metresearch.net/eaquate/Homepage.html].

More specifically, data here analyzed refer to the second day of measurements of the Italian campaign (6th of September) when the Proteus aircraft flew four times over an high cirrus cloud in the Potenza region. High spectral resolution (every 0.24 cm^{-1}) interferometric measurements of the radiance field [-45, +45°] were

collected by the NAST-I sensor covering the long-wave band region 645-2700 cm^{-1}. The cloud evolution was monitored by the DIFA Raman lidar ground station in Potenza by measuring particle backscatter at 355 and 532 nm and extinction at 355 nm. The Raman lidar system also measured water vapour mixing ratio and atmospheric temperature profile. In addition three radiosondes were released from the IMAA ground station (Tito Scalo - Potenza) in 4 hours, and the description of the time evolution of the atmospheric temperature profile and of the atmospheric gaseous and particulate state is therefore excellent. The Proteus aircraft also carried the NAST-M micro-wave radiometer and the S-HIS interferometer.

The objectives of this study are: 1) to co-locate and jointly process data measured by a range of different sensors (Radiosondes/Raman-lidar/NAST-I interferometer); 2) to evaluate the relevance of the lidar information in clear and cloudy sky conditions; 3) to simulate very high spectral resolution interferometric radiances (at different viewing angles) by using a Line-by-Line Multiple Scattering (LbLMS) code and investigate the consistency between measured/modeled radiances in presence of ice clouds; 4) to determine the temporal sequence of the cloud cooling rates and evaluate the importance of the combined lidar–spectrometer information in predicting the evolution of a cirrus cloud, and 5) to set the basis for a study of the evolution of the cirrus cloud accounting for the dynamics and microphysics.

Data Analysis and Results

Ground-based Raman lidar measurements were run almost continuously during the measurement period of the airborne NAST-I interferometer. Lidar provides profile information with accurate information of the statistical measurement uncertainty so that large uncertainties of the lidar-measured parameters may be easily identified and imprecise data can be excluded from further interpretations. Lidar measurement were acquired with a maximum temporal and vertical resolution of 1 min and 30 m, respectively. Vertical and temporal resolution can be traded-off to improve measurement precision. Typical precision for day-time water vapour mixing ratio measurement is 10% at 2 km, while 2 % at 2 km and 20% at 6 km for night-time operation. Typical precision for day-time particle backscatter measurements is 2 % at 2 km, while 1 % up to 5 km and 5 % at 10 km for night-time operation.

The radiosonde temperature profile is used to characterize the atmosphere below flight level during the 4 overpasses. The water vapour mixing ratio profile, obtained from the lidar measurements, is used when the associated percentage error is less than 50% and radiosonde data are used to fill the lidar blind region (60 m above the lidar) and the lidar data affected by large uncertainties. Since the radiance field that has been simulated is the one above the DIFA lidar ground station, the use of the lidar information in defining the water vapour profile, implies a more accurate data in terms of time and location with respect to that obtained from radiosondes.

The rest of the atmospheric column above lidar and radiosondes data is described using the US Standard (USS) atmospheric profile. The concentration profiles for the other molecules (CO_2, O_3, N_2O, CO, CH_4, O_2, NO, SO_2, NO_2 ,N_2, CCl_3F, CCl_2F and CCl_4) are also taken from the USS. The number of levels used for the computation is 94. The number of layers occupied by the cloud is variable and related with the actual cloud geometrical depth measured by the lidar.

Line-by-line computations of layers optical depths are performed using HARTCODE (Rizzi et al., 2002). Single scattering properties for the cloud layers are generated assuming that ice particles are hexagonal columns (Fu et al., 1997; Fu et al., 1998). The cloud optical depths, altitudes and geometrical thickness for the 4 overpasses are determined by the lidar measurements of extinction and back-scattering coefficients. The radiative transfer calculations are performed using the RT3 code, based on adding and doubling method to handle multiple scattering conditions (Amorati and Rizzi, 2001). The code is interfaced with the gaseous and particulate optical depth databases. To simulate accurate interferometric measurements, high spectral resolution radiances are convolved with the appropriate instrumental function.

The NAST-I radiances measured during the 4 overpasses and the DIFA lidar data indicate the presence of an high cirrus cloud whose optical depth is decreasing from the first to the fourth overpass. Lidar backscatter data places cloud top at about 10 km of altitude above the DIFA site, as indicated in Table 1 where a summary of the main features of the cirrus cloud in correspondence to the 4 Proteus overpass Potenza is given..

Table 1: Main features of the cloud as measured by the DIFA Raman lidar

Overpass # (GMT [hh:mm])	**Lowest cloud Limit [km]**	**Upper cloud Limit [km]**	**# of layers**	**Total Optical (Up/Down) Depth at 355 nm**	**Simulated Infrared Transmis. (900 cm^{-1})**
1 (18:02)	6.505	10.065	2	2.45 (1.44 / 1.01)	0.30
2 (18:20)	6.710	10.020	2	0.57 (0.52 / 0.05)	0.75
3 (19:20)	8.450	10.020	2	0.087 (0.073 / 0.014)	0.96
4 (19:40)	8.380	9.230	1	0.0019	0.999

From the data reported it can be noted that the cloud becomes thinner and that the cloud base is raising while the top stays at almost the same level. The lowest of the two layers becomes more transparent as can be inferred from the optical depth values in the fifth column of the same table and during the last overpass the cirrus is almost totally disappeared and the sky can be considered as clear.

Some words need to be used in explaining the geometrical difficulties encountered during the simulation process. In fact, it has to be considered that in every overpass flight altitude was changing and also flight track was different from one pass to another (Proteus never passed on the zenith of the DIFA location). This means that the viewing angle to be considered changes every time since the right field of view (FOV) is the one looking at the top of the cloud over the DIFA for the cloudy scenes, that is about 10 km on its vertical. Moreover, in our computation the airplane rolls has been accounted for since it was quite sensible (reaching the order of some degrees) due to the light weight of aircraft and the high levels' winds. The complication of the entire simulation process is clear if the geometrical complexities are added to those ones usually implied by a LbLMS computation.

NAST-I spectral radiances and brightness temperature (BT) were successfully simulated. The biases in brightness temperature (BT) are less then 4%. Since the percentage error of the difference between the simulated interferometric radiances and the NAST-I data (for everyone of the 4 overpasses) is very low in the whole spectrum, fluxes and heating rates have been computed at all levels at resolution of 0.05 cm^{-1} for every NAST-I overpass of the Potenza region. The results for the spectral cooling rates are shown in Figure 1 where the spectral resolution has been degraded to 20 cm^{-1} for visual purposes. During the first overpass (upper left panel) the cloud is composed of two optically thick layers with a similar optical depth. The high optical depth produces heating at cloud base in the window region. In the far infrared cloud base is still immersed in a quite opaque spectral region determined by the water vapour rotational band. As a consequence, very low values of heating and cooling are detected there. The maximum cooling is observed from 200 to 600 cm^{-1} and in the upper part of the cloud layer.

After 20 minutes (upper right panel) the lower cloud layer has almost disappeared and the window heating takes place at the same altitude of the far infrared cooling. The same situation is found during the third overpass (lower left panel), but the heating and cooling are of lesser magnitude because of the smaller optical depth. During the 4^{th} overpass (lower right panel) the typical features of the clear sky cooling show up. It is interesting to note the cooling structure at 400-600 cm^{-1} and between 2-4 km of altitude in the rotational band of water vapour, a feature not evident in presence of strong down-welling cloud fluxes during the first overpass. The lidar-derived parameters are fundamental in distributing the IWC inside the cloud depth and thus in determining the cooling rates and layers' energy balance.

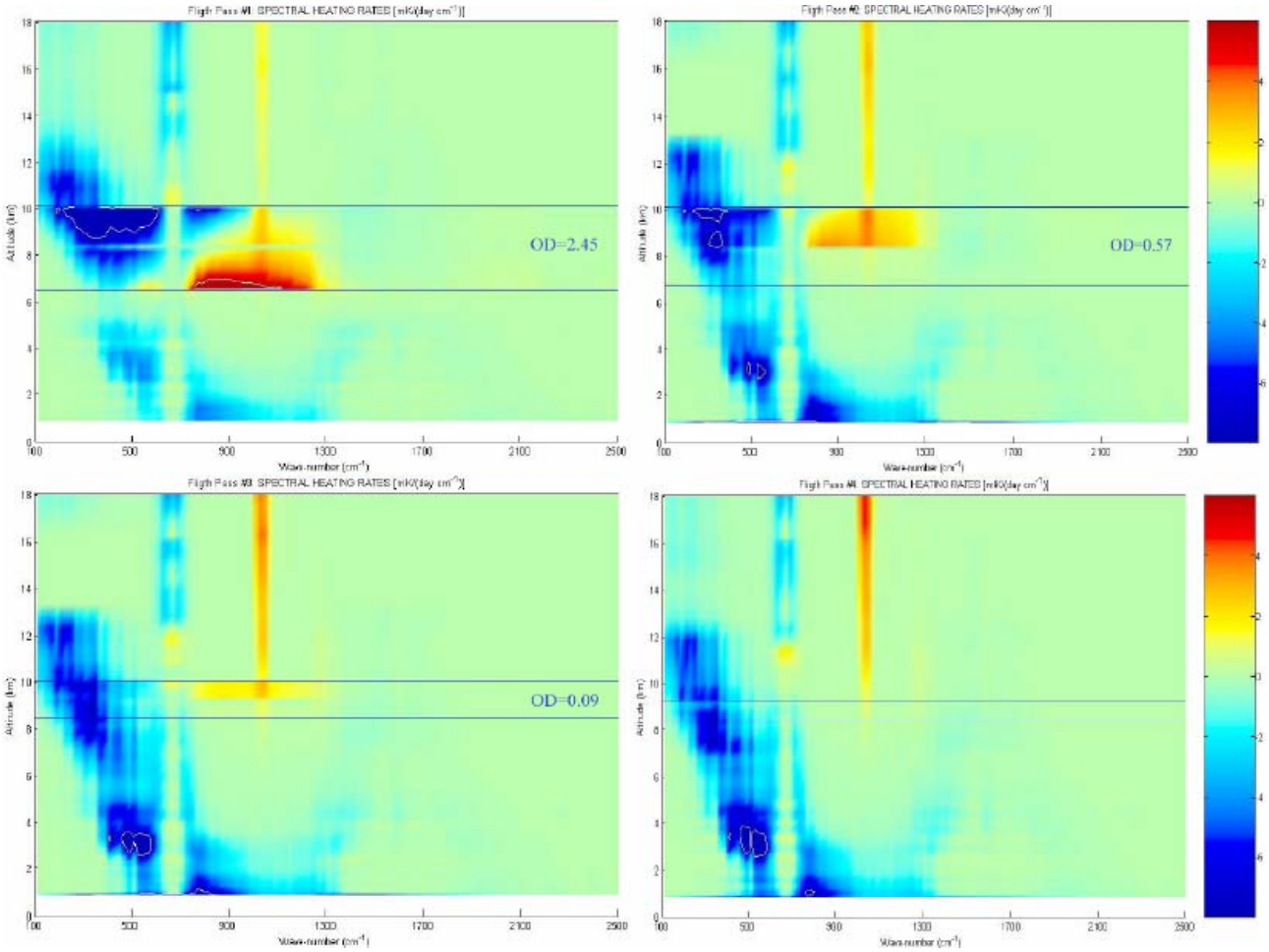

Fig. 1: Spectral cooling rates (averaged on 20 cm^{-1} resolution for visual purposes) in correspondence of the 4 Proteus overpasses the DIFA lidar base. The time sequence is 1st overpass: upper left, 2nd: upper right, 3rd: lower left and 4th: lower right panel. In the firsts 3 panels the measured cloud optical depth (in the short-wave) is also reported.

The total cooling rates computed for the 4 Proteus overpasses over the DIFA site are plotted in Figure 2. The cloud effect is evident both in and out the cloud layers. A sensible gradient between cloud top and bottom is developed only in the first overpass. Nevertheless, the total cooling rates show how the radiative forcing seems to be insufficient to explain the complete cloud dissipation. This is mostly due to the large geometrical thickness (at about 4 km) over which the cloud optical depth is spread. An attenuation of the clear sky cooling below the base cloud level is obtained by the water vapour absorption of the cloud re-emitted and back-scattered infrared radiation. On the second overpass the lower layer of the cloud has almost completely disappeared, causing the window heating and far infrared cooling happening more or less at the same altitude thus strongly compensating each other with the final result of producing a very attenuated cooling peak at the top of the cloud. An interesting cooling feature is obtained for the 4 overpass near the ground level: it can be noted that the cooling of the very low atmospheric levels are less intense with respect to the 2nd and 3rd overpasses. The reason lies in the formation of an inversion layer near the ground with the approach of nighttime.

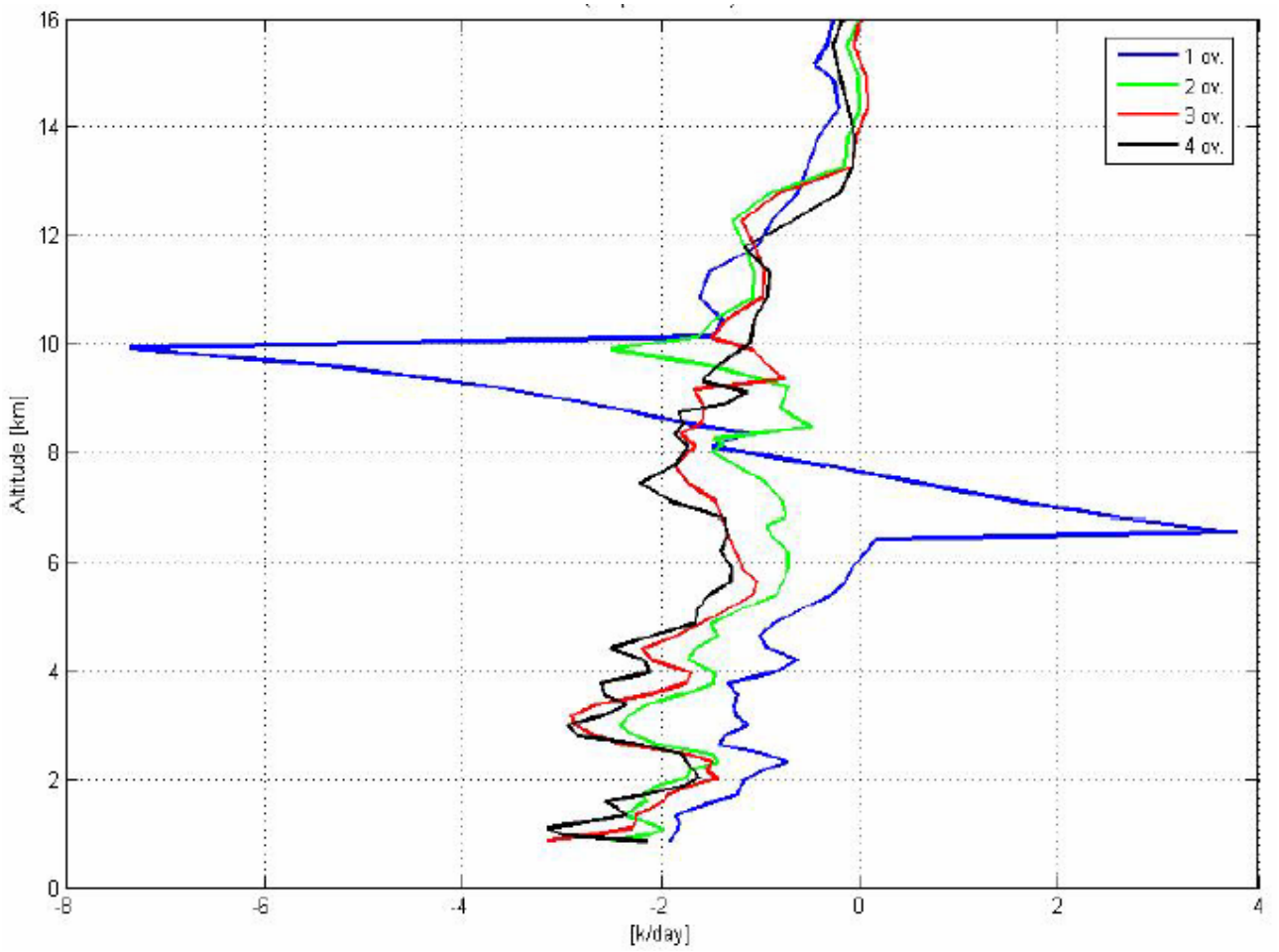

Fig. 2: Total infrared cooling rates (100-2500 cm^{-1}) computed at the four GMT times in correspondence of the Proteus overpasses the Potenza region.

Conclusions and future work

For the case under study the radiative energy exchange does not explain the whole ice cloud sublimation. Microphysics and dynamics need to be accounted for an exhaustive study of a cloud evolution. More lidar information can be used to constrain the simulation (profile of the extinction coefficient, extinction to backscattering ratio, temperature profile) and new cloud particle parameterizations are required to improve consistency between the solar (lidar) and infrared (interferometer) wavelengths.

References

Amorati, R., and R. Rizzi, May 2001, Simulated radiances in presence of clouds using a fast radiative transfer model and a full scattering scheme, submitted to *Applied Optics,* 41(9), 1604-1614.

Fu Q., K. N. Liou, M. C. Cribb, T. P. Charlock, and A. Grossman, 1997, Multiple scattering parameterization in thermal infrared radiative transfer, *Journal of atmospheric Sciences.*, 54, 2799-2812.

Fu Q., Yang Ping, and W. B. Sun, 1998, An accurate parameterization of the infrared radiative properties of cirrus clouds for climate models, *Journal of Climate,* 11, 2223-2237.

Rizzi R., M. Matricardi and F. Miskolczi , On the simulation of up-looking and down-looking high-resolution radiance spectra using two different radiative transfer models, *Applied Optics*, 1-17, 2002.